Med Chem Res (2013) 22:4970–4979
DOI 10.1007/s00044-013-0509-4

MEDICINAL CHEMISTRY RESEARCH

ORIGINAL RESEARCH

Induced-fit docking and binding free energy calculation on furostanol saponins from *Tupistra chinensis* as epidermal growth factor receptor inhibitors

Hua-Jun Luo · Jun-Zhi Wang · Wei-Qiao Deng · Kun Zou

Received: 3 November 2012 / Accepted: 19 January 2013 / Published online: 3 February 2013

Abstract Three furostanol saponins isolated from *Tupistra chinensis* were studied to investigate the reasons for their different inhibitory activities toward non-small-cell lung cancer (NSCLC) A549 cell using induced-fit docking (IFD) between them and epidermal growth factor receptor (EGFR). Their binding free energies were also calculated by molecular mechanics–generalized Born surface area (MM–GBSA) method. The calculation results were all in excellent agreement with experimental activities (IC_{50} values of compound **1–3** against NSCLC A549 cell: 6.6, 6.7, and 29.1 μM). With EGFR (PDB code: 1M17 and 2ITY), the docking IFD score, binding free energy, and binding free energy neglecting the effect of entropy contributions of compound **1** ((25*R*)-26-*O*-β-D-glucopyranosyl-furost-1β,3β,22α,26-tetrahydroxy-3-*O*-β-D-glucopyranoside) were −553.9223, −59.6101, and −70.8088 kcal/mol in 1M17 (−536.2678, −62.2158, and −68.4053 kcal/mol in 2ITY), respectively. The binding sites of compound **1** are similar to erlotinib in 1M17 and gefitinib in 2ITY. There are two hydrogen bonds between compound **1** and the key amino acid residue Met769 in 1M17 or Met793 in 2ITY. The only structure difference between compound **3** and compound **1** is 5-hydroxyl polar group in compound **3**, which hinders the hydrophobic interactions with EGFR and increases polar solvation free energy term that opposes binding. This indicates that compound **1** could be a potent EGFR inhibitor for NSCLC treatment.

Keywords Furostanol saponins · Induced-fit docking · EGFR · Binding free energy

Introduction

Kaikoujian, the Chinese name of rhizomes of *Tupistra chinensis* BAK., belongs to the family Liliaceae (Convallarieae) (Zou *et al*., 2006). As a reputed folk medicine in Shennongjia Forest District of China, kaikoujian has been used to reduce carbuncles and to ameliorate pharyngitis (Zhan, 1994; Liu *et al*., 2012a, b). Recently, three furostanol saponins (compound **1**, (25*R*)-26-*O*-β-D-glucopyranosyl-furost-1β,3β,22α,26-tetrahydroxy-3-*O*-β-D-glucopyranoside; compound **2**, (25*R*)-26-*O*-β-D-glucopyranosyl-furost-1β,3α,22α,26-tetrahydroxy-5(6)-en-3-*O*-β-D-glucopyranoside; and compound **3**, (25*R*)-26-*O*-β-D-glucopyranosyl-furost-1β,3β,5β,22α,26-pentahydroxy-3-*O*-β-D-glucopyranoside) were isolated from kaikoujian by our group (Zou *et al*., 2009; Guo *et al*., 2009; Liu *et al*., 2012a) (Fig. 1). Using the MTT assay method, compounds **1**, **2**, and **3** showed cytotoxicity against non-small-cell lung cancer (NSCLC) A549 cell lines with IC_{50} values of 6.6, 6.7, and 29.1 μM (Liu *et al*., 2012a), respectively.

Protein tyrosine kinases (PTKs) catalyze the phosphorylation of tyrosine residues in various proteins and play pivotal roles in cell regulation, including proliferation, differentiation, cell cycle progression, angiogenesis, and the inhibition of apoptosis (Lv *et al*., 2011; Paul and Mukhopadhyay, 2004). PTKs can be classified into two classes: receptor tyrosine kinases and non-receptor tyrosine

H.-J. Luo · J.-Z. Wang · K. Zou (✉)
Hubei Key Laboratory of Natural Products Research and Development, College of Chemistry & Life Science, China Three Gorges University, Yichang 443002, Hubei, China
e-mail: kzou_ctgu@163.com

H.-J. Luo
e-mail: luohuajun@21cn.com

W.-Q. Deng
Dalian Institute of Chemical Physics, Chinese Academy of Sciences, Dalian 116023, Liaoning, China

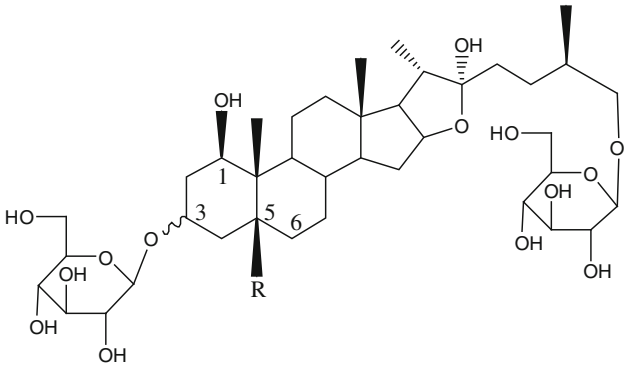

1 R=H 3β
2 $\Delta^{5(6)}$ 3α
3 R=OH 3β

Fig. 1 The chemical structures of compounds **1–3**

kinases. The human epidermal growth factor receptor (EGFR) is a trans-membrane receptor tyrosine kinase that belongs to the HER family of receptors, which consists of a single polypeptide chain of 1,186 amino acids (Bishayee, 2000; Ogiso *et al*., 2002). The EGFR plays an essential role in normal organ development by mediating morphogenesis and differentiation (Li *et al*., 2012a, b). Deregulation of EGFR activity is extremely associated with tumor formation, such as lung cancer, breast cancer, ovarian cancer, and so on (Hynes *et al*., 2001; Kuan *et al*., 2001; Dutta and Maity, 2007; de Oliveira *et al*., 2010). Therefore, EGFR is a key anti-tumor target. Now non-small-cell lung cancer is one of the most common causes of cancer death worldwide. There are various reports that EGFR is a cause of mostly NSCLC (Choong *et al*., 2005; Baselga and Arteaga, 2005; Herbst *et al*., 2004; Cho *et al*., 2007). So the objectives of this article were to propose the furostanol saponins from *Tupistra chinensis* as EGFR inhibitors using induced-fit docking (IFD) method to investigate the binding sites between three furostanol saponins and EGFR, and calculate their binding free energies by molecular mechanics–generalized Born surface area (MM–GBSA) method.

Materials and methods

Protein structure preparation

The atomic co-ordinates for the structure of EGFR were downloaded from the Protein Data Bank (PDB codes: 1M17 and 2ITY) (Stamos *et al*., 2002; Yun *et al*., 2007). The subsequent 1M17 and 2ITY models were subject to the Protein Preparation Wizard module in Schrödinger as follows: adding hydrogen, assigning partial charges using the OPLS-2001 force field, and assigning protonation states. All crystal waters were removed. Then the minimization was carried out using the OPLS force field in the MacroModel module in Schrödinger (Schrödinger, 2010) with backbone atoms being fixed.

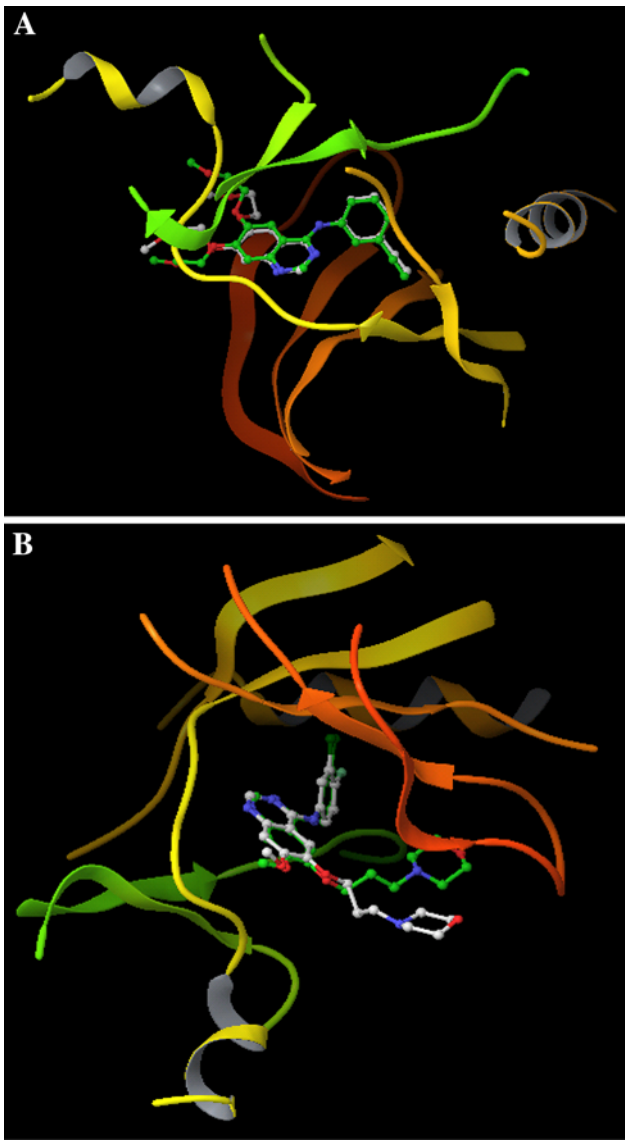

Fig. 2 **a** The binding sites of 1M17 with erlotinib: native erlotinib (*gray carbons*), IFD-generated erlotinib model (*green carbons*). **b** The binding sites of 2ITY with gefitinib: native gefitinib (*gray carbons*), IFD-generated gefitinib model (*green carbons*)

Compound preparation

Compounds were built by Maestro-molecular builder. LigPrep of Schrödinger software suit (Schrödinger, 2010) was used for final preparation of ligands: generating 3D structures from 1D (Smiles) and 2D (SDF) representation, searching for steric isomers, and performing a geometry

Table 1 Calculated glide Gscores, IFD scores, and binding free energies for EGFR–ligand complexes using MM–GBSA

	1M17				2ITY			
	1	**2**	**3**	Erlotinib	**1**	**2**	**3**	Gefitinib
Glide Gscore	−9.6668	−9.3102	−8.6177	−8.7729	−10.1093	−9.6630	−8.4504	−8.1959
IFD score	−553.9223	−553.3129	−552.3241	−561.5343	−536.2678	−536.1061	−535.1994	−544.2100
$\Delta E_{\text{internal}}$ (kcal/mol)	−0.0310	−0.0150	−0.0071	0	0	0	0	0
ΔE_{Elect} (kcal/mol)	−47.5585	−61.3695	−64.4172	−25.6842	−58.2678	−55.5934	−56.3784	−17.3752
ΔE_{VDW} (kcal/mol)	−59.5416	−60.3236	−67.1088	−54.1882	−47.4999	−65.8628	−58.6812	−51.9768
ΔG_{GB} (kcal/mol)	43.5462	55.5890	70.8792	23.9948	40.7993	64.3095	61.9042	23.6187
ΔG_{SA} (kcal/mol)	−7.2238	−4.1491	−0.8451	−1.5948	−3.6963	−4.5891	0.5981	−3.2371
$T\Delta S$ (kcal/mol)	−11.1987	−15.6203	−11.1613	−2.8178	−6.1895	−13.4260	−8.2872	−3.5751
$\Delta G'_{\text{bind}}$ (kcal/mol)	−70.8088	−70.2682	−61.4990	−57.4723	−68.4053	−61.7358	−52.5573	−48.9704
ΔG_{bind} (kcal/mol)	−59.6101	−54.6480	−50.3377	−54.6545	−62.2158	−48.3098	−44.2701	−45.3953

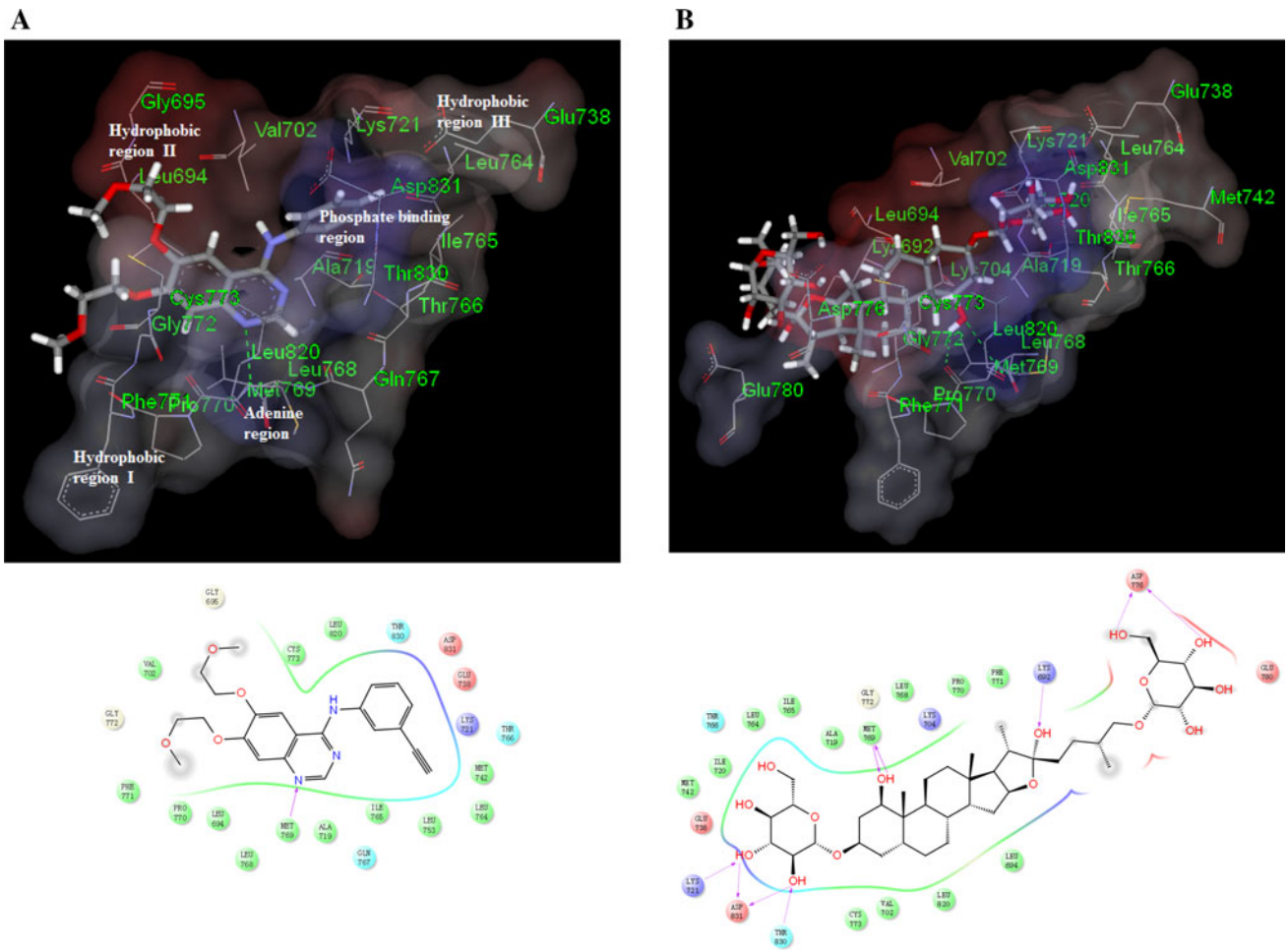

Fig. 3 The binding sites of ligands with EGFR (1M17) **a** erlotinib, **b** compound **1**, **c** compound **2**, and **d** compound **3**

minimization of ligands. The ligands were subjected to energy minimization using MacroModel module of Schrödinger with Merck Molecular Force Field (MMFFs). Truncated Newton Conjugate Gradient (TNCG) minimization method was used with 500 iterations and convergence threshold of 0.05 (kJ/mol).

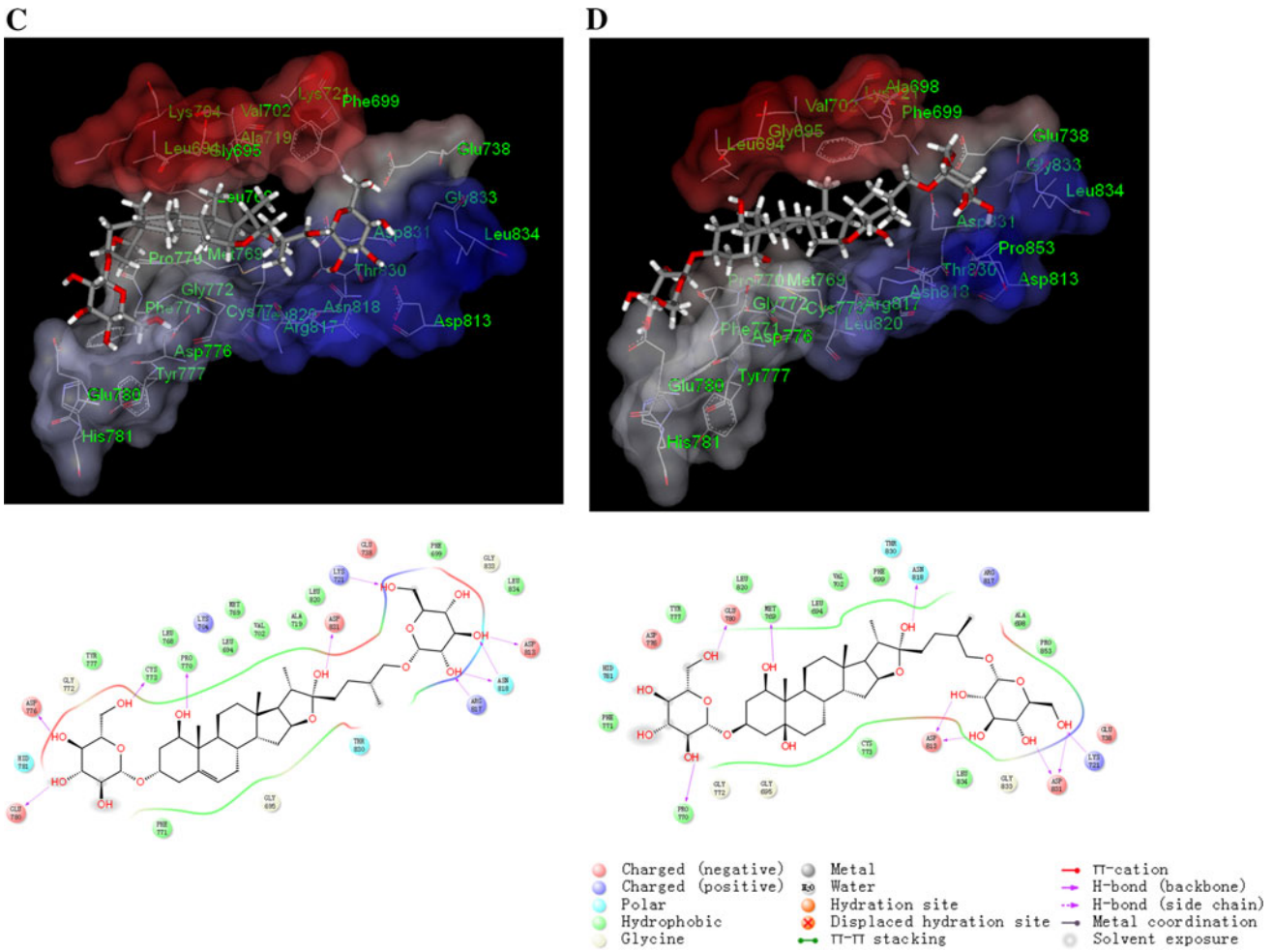

Fig. 3 continued

Induced-fit docking

Molecular docking simulation was performed using induced-fit docking (IFD) method (Sherman *et al*., 2006) in the Schrödinger software suite (Schrödinger, 2010), which had been reported to be a robust and accurate method to account for both ligand and receptor flexibility (Sherman *et al*., 2006; Zhong *et al*., 2009). The EGFR plasticity is taken into account in the IFD by iteratively combining rigid receptor docking using Glide program (Friesner *et al*., 2004) with sampling side chain degrees of freedom in the receptor while allowing minor backbone movements through the minimization using the Prime program (Jacobson *et al*., 2004) in the Schrödinger suite.

The IFD protocol was carried out in three consecutive steps (Wanga *et al*., 2008). First, the ligand was docked into a rigid receptor model with scaled-down van der Waals (vdW) radii. A vdW scaling of 0.5 was used for both the protein and ligand non-polar atoms. A constrained energy minimization was carried out on the protein structure using the OPLS-2001 force field. The Glide SP mode was used for the initial docking, and 20 ligand poses were retained for protein structural refinements. The docking box was defined to include all amino acid residues within the dimensions of 30 Å × 30 Å × 30 Å from the center of the ligand (erlotinib in 1M17 or gefitinib in 2ITY). Second, Prime program was used to generate the induced-fit protein–ligand complexes. Each of the 20 structures from the previous step was subjected to side chain and backbone refinements. All residues with at least one atom located within 5.0 Å of each corresponding ligand pose were included in the Prime refinement. The refined complexes were ranked by Prime energy, and the receptor structures within 30 kcal/mol of the minimum energy structure were passed through for a final round of Glide docking and scoring. Finally, each ligand was redocked into every refined low-energy receptor structure produced in the second step using Glide SP mode at default settings. An

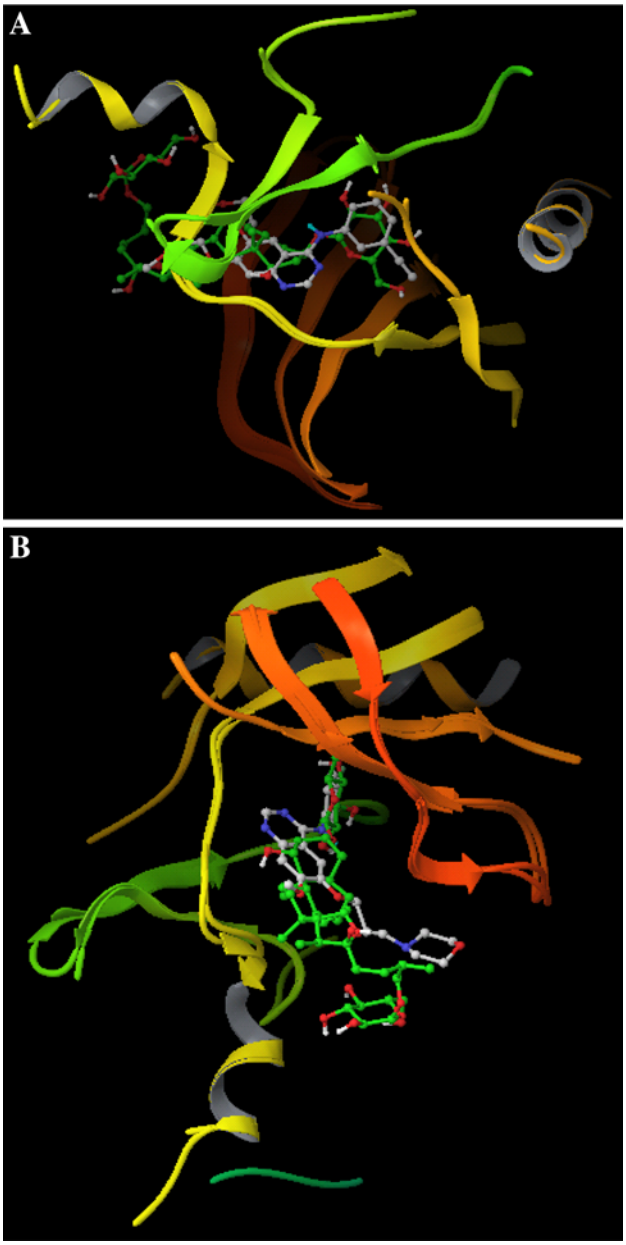

Fig. 4 **a** The binding sites of EGFR (1M17) with native erlotinib (*gray carbons*) and IFD-generated compound **1** model (*green carbons*). **b** The binding sites of EGFR (2ITY) with native gefitinib (*gray carbons*) and IFD-generated compound **1** model (*green carbons*)

IFD score (IFD score = 1.0 Glide_Gscore + 0.05 Prime_Energy) that accounts for both the protein–ligand interaction energy and the total energy of the system was calculated and used to rank the IFD poses. The more negative IFDscore, the more favorable the binding. The best pose of ligand–protein complexes was visualized using PyMOL0.99 (De Lano, 2004) and analyzed by Ligand Interactions module embedded in Maestro 9.3 (Maestro, 2012).

Table 2 The hydrogen bond interactions between the ligands and residues of EGFR (1M17)

Compounds	Atoms	Residues	Atoms	Distance (Å)
1	O4	Lys692	HZ3	2.25
	O8	Lys721	HZ1	2.04
	O15	Met769	H	2.18
	H66	Met769	O	2.11
	H62	Asp776	OD2	1.80
	H63	Asp776	OD2	2.18
	O9	Thr830	HG1	2.22
	H53	Asp831	OD2	1.80
	H54	Asp831	OD2	1.81
2	O11	Lys721	HZ3	1.83
	H64	Pro770	O	1.83
	H49	Cys773	O	1.93
	H50	Asp776	O	1.63
	H51	Glu780	OE2	1.56
	H62	Asp813	OD2	1.96
	O14	Arg817	HH11	1.93
	O13	Asn818	HD22	1.81
	H63	Asn818	OD1	1.91
	H30	Asp831	OD2	1.92
3	O11	Lys721	HZ3	2.33
	H65	Met769	O	1.93
	H53	Pro770	O	1.66
	H50	Glu780	OE1	1.83
	H64	Asp813	OD2	2.46
	H31	Asn818	OD1	1.99
	H62	Asp831	OD1	1.78
	H63	Asp831	OD2	2.20

MM–GBSA calculation

Molecular mechanics–generalized Born surface area (MM–GBSA) is emerging as a useful and effective approach to predict the binding free energy (ΔG_{bind}). The results showed that correlations between MM–GBSA binding free energies with experimental affinities were in most cases in excellent agreement. Importantly the correlations obtained with the use of a single protein–ligand minimized structure and with implicit solvation models were similar to those obtained after averaging over multiple molecular dynamics snapshots with explicit water molecules, with consequent save of computing time without loss of accuracy (Ahmedm *et al*., 2010). MM–GBSA procedure in Prime program (Jacobson *et al*., 2004; Kollman *et al*., 2011) was used to calculate ΔG_{bind} of the docked inhibitors according to the following equations (Massova and Kollman, 2000):

$$\Delta G'_{bind} = \Delta E_{MM} + \Delta G_{solv} \quad (1)$$

$$\Delta G_{bind} = \Delta E_{MM} + \Delta G_{solv} - T\Delta S \quad (2)$$

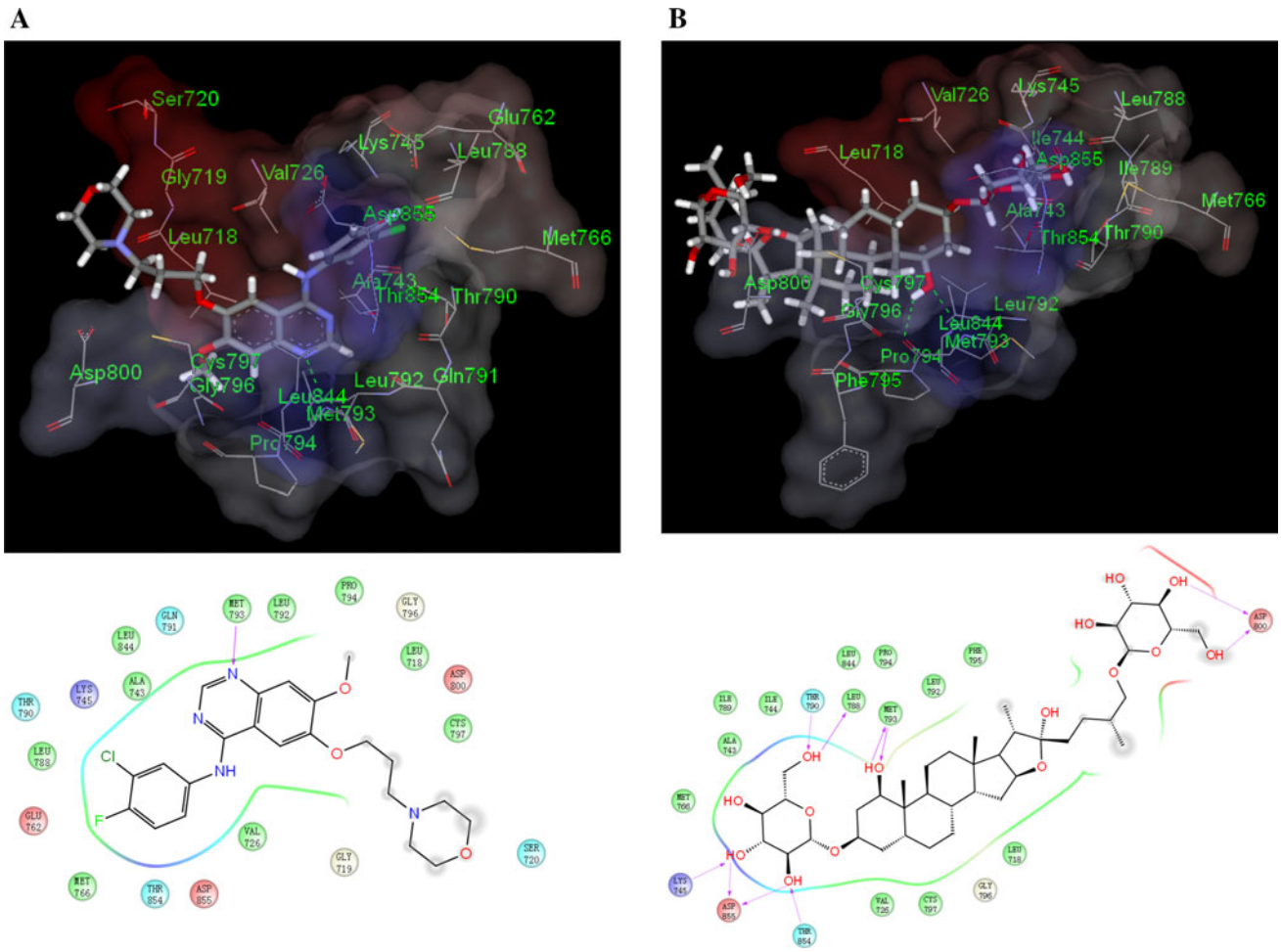

Fig. 5 The binding sites of ligands with EGFR (2ITY) **a** gefitinib, **b** compound **1**, **c** compound **2**, and **d** compound **3**

where ΔE_{MM} is the difference of the gas phase MM energy between the complex and the sum of the energies of the EGFR and inhibitor, and includes $\Delta E_{internal}$ (bond, angle, and dihedral energies), ΔE_{Elect} (electrostatic), and ΔE_{VDW} (van der Waals) energies. ΔG_{solv} is the change of the solvation free energy upon binding, and includes the electrostatic solvation free energy ΔG_{GB} (polar contribution calculated using generalized Born model), and the nonelectrostatic solvation component ΔG_{SA} (nonpolar contribution estimated by solvent accessible surface area). $T\Delta S$ is the change of the conformational entropy upon binding. This term was calculated using normal-mode analysis Rigid Rotor Harmonic Oscillator (RRHO) contained in MacroModel module (Schrödinger, 2010; Kaminski *et al*., 2001). $\Delta G'_{bind}$ neglects the effect of entropy contributions, while ΔG_{bind} includes contributions from loss of ligand translational, rotational, and vibrational entropy ($T\Delta S$).

Results and discussion

The validation of IFD model was performed before docking simulation. The superposition of the IFD-generated erlotinib model (carbons in green, Fig. 2a) to the native structure of erlotinib (carbons in gray, Fig. 2a) in erlotinib/EGFR complex (1M17) yielded a RMSD of 1.49 Å for all heavy atoms (excluding the hydrogen atoms). The RMSD of the core structures (all heavy atoms excluding the 2-methoxyethoxy moiety) between the IFD model and the native erlotinib in 1M17 is 0.21 Å. The RMSD of all heavy atoms between the IFD-generated gefitinib and the native pose in 2ITY was 2.18 Å (Fig. 2b). Excluding the 3-morpholin-4-ylpropoxy moiety, the RMSD of core structures between two gefitinib molecules was 0.27 Å. Obviously, the IFD-generated erlotinib and gefitinib models are very close to the native ligands in the crystal 1M17 and 2ITY.

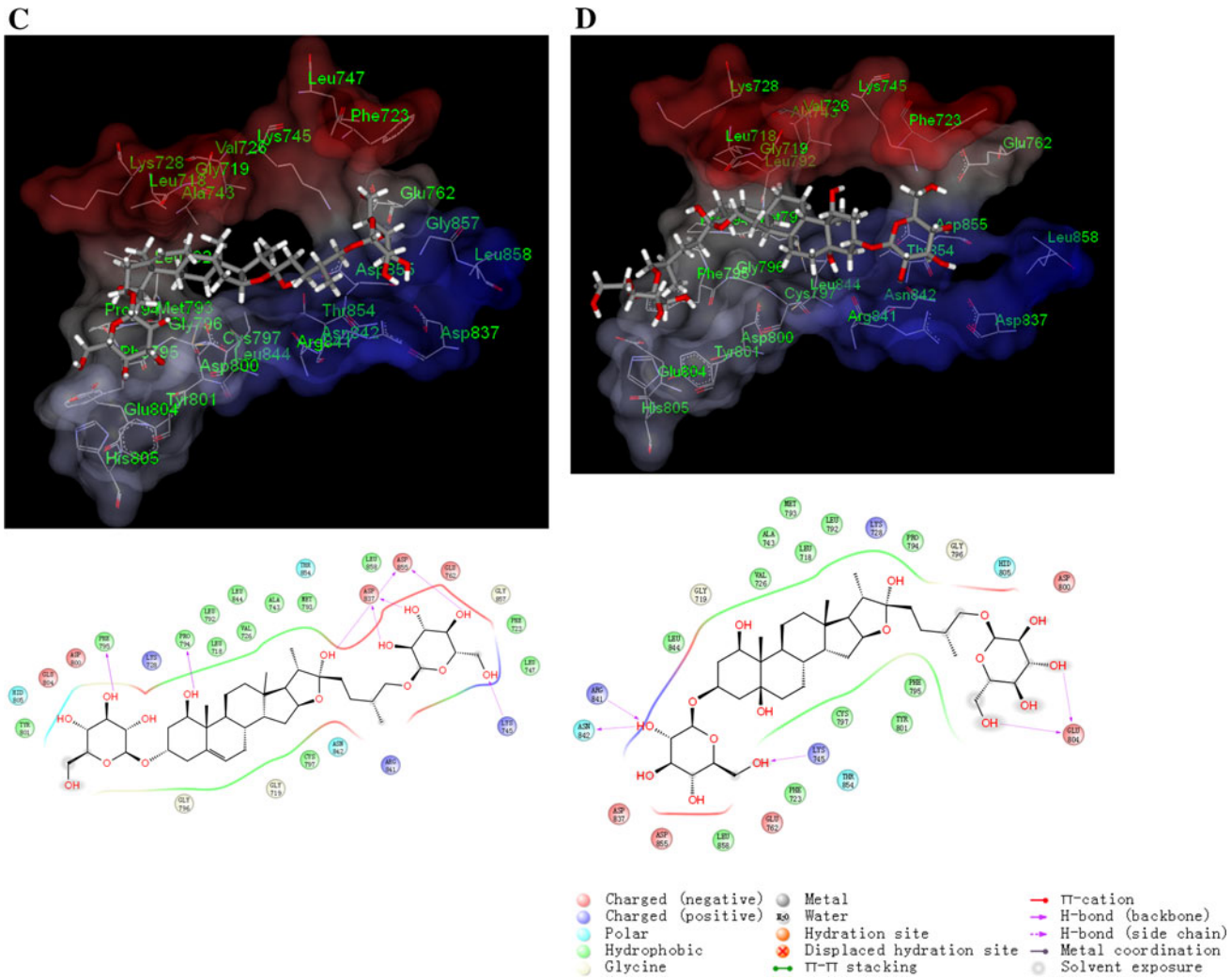

Fig. 5 continued

The validation results are in agreement with the reference (Zhong *et al.*, 2009). So the IFD module could be applied to predict the binding interactions between compounds and EGFR.

Then molecular docking between furostanol saponins and EGFR was simulated by IFD method. The Glide Gscores and IFD scores of compound **1**–**3** (the best pose in 1M17 and 2ITY) were shown in Table 1. The correlation between IFD scores and experimental activities (IC_{50} values) was in excellent agreement. The docking affinity of compound **1** (IFD score_1M17 = −553.9223; IFD score_2ITY = −536.2678) is better than compound **2** (IFD score_1M17 = −553.3129; IFD score_2ITY = −536.1061) and **3** (IFD score_1M17 = −552.3241; IFD score_2ITY = −535.1994).

Based on an examination of the crystal structure of 1M17 (Lv *et al.*, 2011; Sawatdichaikul *et al.*, 2012), one nitrogen atom of the quinazoline skeleton in erlotinib forms a strong hydrogen bond with Met769 (the distance: 1.61 Å) in adenine region of EGFR (Fig. 3a). Erlotinib also shows lipophilic stacking interactions with the residues in hydrophobic pocket region I (Pro 770, Phe771, Cys773), hydrophobic region II (Leu694, Val702), and hydrophobic region III (Leu764, Ile765). Lys721 interacts with erlotinib through positive charged interaction, while there is negative charged interaction with Asp831 in phosphate binding region of EGFR (Fig. 3a). The binding sites of compound **1** are similar to erlotinib (Fig. 4a). Compound **1** interacts with Lys692, Lys721, Met769, Asp776, Thr830, and Asp831 of EGFR via hydrogen bonds (Fig. 3b; Table 2). Meanwhile, Lys721 and Asp831 play the same role in charged interaction as erlotinib. There are also hydrophobic interactions between compound **1** and residues Leu694, Val702, Ala719, Ile720, Met742, Leu764, Ile765, Leu768, Pro770, Phe771, Cys773, and Leu820. Especially 5, 6-site atoms of compound **1** are in hydrophobic pocket region II interacting with Val702 (Fig. 3b). There are some strong hydrogen bonds between

Table 3 The hydrogen bond interactions between the ligands and residues of EGFR (2ITY)

Compounds	Atoms	Residues	Atoms	Distance (Å)
1	O8	Lys745	HZ2	1.93
	H51	Leu788	O	1.82
	O6	Thr790	HG1	2.32
	O15	Met793	H	2.10
	H66	Met793	O	2.19
	H62	Asp800	OD2	1.82
	H63	Asp800	OD2	2.08
	O9	Thr854	HG1	2.13
	H53	Asp855	OD1	1.83
	H54	Asp855	OD1	1.90
2	O11	Lys745	HZ1	2.01
	H64	Pro794	O	1.90
	H51	Phe795	O	1.96
	H62	Asp837	OD2	2.23
	H63	Asp837	OD2	1.97
	H30	Asp855	OD1	1.61
	H61	Asp855	OD2	1.86
3	O6	Lys745	HZ1	1.97
	H61	Glu804	OE2	1.87
	H63	Glu804	OE1	1.68
	O9	Arg841	HH11	1.95
	H53	Asn842	OD1	1.64

compound **2** and Lys721, Pro770, Cys773, Asp776, Glu780, Asp813, Arg817, Asn818, and Asp831 (Fig. 3c; Table 2), but not including the key amino acid residue Met769. Although the 1-hydroxyl group of compound **3** makes the hydrogen bond interaction with Met769 (distance: 1.93 Å), 5-hydroxyl group of compound **3** hinders the hydrophobic interactions with hydrophobic region II of EGFR (Fig. 3d).

The superposition of IFD-generated compound **1** and gefitinib in EGFR (2ITY) was shown in Fig. 4b. The binding sites of compound **1** are also similar to gefitinib. The crystal structure of 2ITY shows that gefitinib forms a strong hydrogen bond with Met793 (the distance: 1.70 Å) in adenine region of EGFR (Fig. 5a), and interacts with the residues in hydrophobic pocket region (Pro794, Cys797, Leu718, Val726, Met766, and Leu788). Compound **1** forms hydrogen bonds with Met793 in EGFR (2ITY) (the distance: 2.10 and 2.19 Å), and other residues Lys745, Leu788, Thr790, Asp800, Thr854, and Asp855 (Fig. 5b; Table 3). There are hydrophobic interactions between compound **1** and residues Leu718, Val726, Ala743, Ile744, Met766, Leu788, Ile789, Leu792, Pro794, Phe795, and Cys797 (Fig. 5b). Atoms in 5, 6-site of compound **1** also interact with Val726 in hydrophobic pocket. As listed in Table 3, the hydrogen bond number of compound **2** (compound **3**) with EGFR (2ITY) is less than that of compound **1**, and the key amino acid residue Met793 in 2ITY does not interact with compound **2** and compound **3** (Fig. 5c, d). 1-Hydroxyl group and 5-hydroxyl group (the polar group) of compound **3** are in hydrophobic region (Val726 and Cys797) (Fig. 5d), which hinders the hydrophobic interactions with EGFR.

Zhong *et al*. (2009) reported that residues important for the EGFR binding include Lys745, Thr790, Met793, and Cys797 (2ITY), and suggested that Cys797 should be taken into account in drug design targeting the EGFR. By in silico screening of EGFR inhibitors, Sawatdichaikul *et al*. (2012) found that it is the most important hydrogen bonding with Met769 (1M17), and Lys721 that plays a significant role interacting with candidates. Hence, based on above docking analysis, compound **1** could be a potent EGFR inhibitor. The EGFR inhibitory activity of compound **3** is lower than that of compound **1**, which indicates that 5-site of furostanol saponin should not have the polar group for high activity.

The binding free energy values obtained from MM–GBSA calculations were reported in Table 1. The $\Delta G'_{\text{bind}}$ and ΔG_{bind} values all showed that the favorable order of interaction is compound **1** > **2** > **3** (in 1M17, ΔG_{bind} of compound **1** was −59.6101 kcal/mol, and the difference in the calculated ΔG_{bind} value between compound **1** and **3** was −9.2724 kcal/mol; in 2ITY, ΔG_{bind} of compound **1** was −62.2158 kcal/mol, and the difference in the calculated ΔG_{bind} value between compound **1** and **3** was −17.9457 kcal/mol). ΔG_{bind} and $\Delta G'_{\text{bind}}$ absolute values of compound **1** are all higher than erlotinib and gefitinib. According to the energy components of the binding free energies (Table 1), the major favorable contributors to ligand binding are ΔE_{VDW} and ΔE_{Elect} terms, whereas polar solvation (ΔG_{GB}) and entropy terms oppose binding. Nonpolar solvation terms contribute favorably for the complex with compound **1** ($\Delta G_{\text{SA}} = -7.2238$ kcal/mol in 1M17; $\Delta G_{\text{SA}} = -3.6963$ kcal/mol in 2ITY) and slightly favorably or unfavorably for the complex with compound **3** ($\Delta G_{\text{SA}} = -0.8451$ kcal/mol in 1M17; $\Delta G_{\text{SA}} = 0.5981$ kcal/mol in 2ITY). If we examine the contributions to each binding energy, the most important term which dictates the difference in the binding affinity is ΔG_{GB}. The better binding of compound **1** gains over −27.3330 (−21.1049) kcal/mol of ΔG_{GB} value compared with compound **3** in 1M17 (2ITY). This is in agreement with the docking results previously: compound **1** has the best inhibitory activity against EGFR among three furostanol saponins.

Conclusions

The reasons for the different NSCLC A549 cell inhibitory activities of three furostanol saponins isolated from kaikoujian were studied using induced-fit docking with EGFR

and MM–GBSA binding free energy calculation methods. The calculation results were in excellent agreement with experimental activities order: compound **1** > **2** > **3**. The docking Gscore, IFD score, ΔG_{bind} and, $\Delta G'_{bind}$ values of compound **1** were −9.6668, −553.9223, −59.6101, and −70.8088 kcal/mol in 1M17 (−10.1093, −536.2678, −62.2158, and −68.4053 kcal/mol in 2ITY), respectively. Compound **1** ((25*R*)-26-*O*-β-D-glucopyranosyl-furost-1β, 3β,22α,26-tetrahydroxy-3-*O*-β-D-glucopyranoside) interacts with Lys692, Lys721, Met769, Asp776, Thr830, and Asp831 of EGFR (1M17) via hydrogen bonds. There are also hydrophobic interactions between compound **1** and residues Leu694, Val702, Ala719, Ile720, Met742, Leu764, Ile765, Leu768, Pro770, Phe771, Cys773, and Leu820 in 1M17. Especially 5, 6-site atoms of compound **1** are in hydrophobic pocket region interacting with Val702. The docking results of furostanol saponins with EGFR (2ITY) were similar to those with 1M17. The structure difference between compound **3** and compound **1** is 5-hydroxyl polar group in compound **3**, which hinders the hydrophobic interactions with EGFR and increases polar solvation free energy term ΔG_{GB} that opposes binding. Thus, the interaction is more favorable for compound **1**-EGFR complex and compound **1** could be a potent EGFR inhibitor. However, further pharmacological study would be necessary to confirm the calculation conclusions.

Acknowledgments This work was Granted by National Natural Science Foundation of China (No. 30760213, 30870254) and Science Foundation of China Three Gorges University (No. KJ2010B001).

References

Ahmedm S, Metpally RPR, Sangadala S, Reddy BVB (2010) Virtual screening and selection of drug-like compounds to block noggin interaction with bone morphogenetic proteins. J Mol Graph Model 28:670–682

Baselga J, Arteaga CL (2005) Critical update and emerging trends in epidermal growth factor receptor targeting in cancer. J Clin Oncol 23:2445–2459

Bishayee S (2000) Role of conformational alteration in the epidermal growth factor receptor (EGFR) function. Biochem Pharmacol 60:1217–1223

Cho BC, Im CK, Park MS, Kim SK, Chang J, Park JP, Choi HJ, Kim YJ, Shin SJ, Sohn JH, Kim H, Kim JH (2007) Phase II study of erlotinib in advanced non-small-cell lung cancer after failure of gefitinib. J Clin Oncol 25:2528–2533

Choong NW, Ma PC, Salgia R (2005) Therapeutic targeting of receptor tyrosine kinases in lung cancer. Expert Opin Ther Targets 9:533–559

De Lano WL (2004) The PyMOL molecular graphics system. DeLano Scientific LLC, San Carlos. http://pymol.sourceforge.net. Accessed 1 June 2004

de Oliveira AN, Bocca CC, Carvalho JE, Ruiz ALG, Silva TP, Rittner R, Hoehr NF (2010) New substituted 4-arylaminoquinazolines as potent inhibitors of breast tumor cell lines: in vitro and docking experiments. Eur J Med Chem 45:4339–4342

Dutta PR, Maity A (2007) Cellular responses to EGFR inhibitors and their relevance to cancer therapy. Cancer Lett 254:165–177

Friesner RA, Banks JL, Murphy RB, Halgren TA, Klicic JJ, Mainz DT, Repasky MP, Knoll EH, Shelley M, Perry JK, Shaw DE, Francis P, Shenkin PS (2004) Glide: a new approach for a rapid, accurate docking and scoring. 1. Method and assessment of docking accuracy. J Med Chem 47:1739–1749

Guo ZY, Zou K, Wang JZ, Liu C, Tang ZC, Yang CY (2009) Structural elucidation and NMR spectral assignment of three new furostanol saponins from the roots of *Tupistra chinensis*. Magn Reson Chem 47:613–616

Herbst RS, Fukuoka M, Baselga J (2004) Gefitinib—a novel targeted approach to treating cancer. Nat Rev Cancer 4:956–965

Hynes N, Horsch K, Olayioye M, Badache A (2001) The ErbB receptor tyrosine family as signal integrators. Endocr Relat Cancer 8:151–159

Jacobson MP, Pincus DL, Rapp CS, Day TJF, Honig B, Shaw DE, Friesner RA (2004) A hierarchical approach to all-atom protein loop prediction. Proteins 55:351–367

Kaminski GA, Friesner RA, Tirado-Rives J, Jorgensen WL (2001) Evaluation and reparametrization of the OPLS-AA force field for proteins via comparison with accurate quantum chemical calculations on peptides. J Phys Chem B 105:6474–6487

Kollman PA, Massova I, Reyes C, Kuhn B, Huo S, Chong L (2011) Calculating structures and free energies of complex molecules: combining molecular mechanics and continuum models. Acc Chem Res 33:889–897

Kuan C, Wikstrand C, Bigner D (2001) EGF mutant receptor vIII as a molecular target in cancer therapy. Endocr Relat Cancer 8:83–96

Li SY, Guo CY, Sun XQ, Li YZ, Zhao HL, Zhan DM, Lan MB, Tang Y (2012a) Synthesis and biological evaluation of quinazoline and quinoline bearing 2,2,6,6-tetramethylpiperidine-*N*-oxyl as potential epidermal growth factor receptor(EGFR) tyrosine kinase inhibitors and EPR bio-probe agents. Eur J Med Chem 49:271–278

Li SY, Guo CY, Zhao HL, Tang Y, Lan MB (2012b) Synthesis and biological evaluation of 4-[3-chloro-4-(3-fluorobenzyloxy) anilino]-6-(3-substituted-phenoxy)pyrimidines as dual EGFR/ErbB-2 kinase inhibitors. Bioorg Med Chem 20:877–885

Liu CX, Guo ZY, Xue YH, Cheng J, Huang NY, Zhou Y, Cheng F, Zou K (2012a) Five new furostanol saponins from the rhizomes of *Tupistra chinensis*. Fitoterapia 83:323–328

Liu CX, Guo ZY, Xue YH, Zhang HY, Zhang HQ, Zou K, Huang NY (2012b) Tupisteroide A-C, three new polyhydroxylated steroidal constituents from the roots of *Tupistra chinensis*. Magn Reson Chem 50:320–324

Lv PC, Li DD, Li QS, Lu X, Xiao ZP, Zhu HL (2011) Synthesis, molecular docking and evaluation of thiazolyl-pyrazoline derivatives as EGFR TK inhibitors and potential anticancer agents. Bioorg Med Chem Lett 21:5374–5377

Maestro, version 9.3, Schrödinger, LLC, New York (2012). www.schrodinger.com. Accessed 23 Jan 2012

Massova I, Kollman PA (2000) Combined molecular mechanical and continuum solvent approach (MM–PBSA/GBSA) to predict ligand binding. Perspect Drug Discov Des 18:113–135

Ogiso H, Ishitani R, Nureki O, Fukai S, Yamanaka M, Kim JH, Saito K, Sakamoto A, Inoue M, Shirouzu M, Yokoyama S (2002) Crystal structure of the complex of human epidermal growth factor and receptor extracellular domains. Cell 110:775–787

Paul MK, Mukhopadhyay AK (2004) Tyrosine kinase—role and significance in cancer. Int J Med Sci 1:101–115

Sawatdichaikul O, Hannongbua S, Sangma C, Wolschann P, Choowongkomon K (2012) In silico screening of epidermal growth factor receptor (EGFR) in the tyrosine kinase domain through a medicinal plant compound database. J Mol Model 18(3):1241–1254

Schrödinger, LLC, New York (2010). www.schrodinger.com. Accessed 1 Oct 2010

Sherman W, Day T, Jacobson MP, Friesner RA, Farid R (2006) Novel procedure for modeling ligand/receptor induced fit effects. J Med Chem 49:534–553

Stamos J, Sliwkowski MX, Eigenbrot C (2002) Structure of the epidermal growth factor receptor kinase domain alone and in complex with a 4-anilinoquinazoline inhibitor. J Biol Chem 277:46265–46272

Wanga H, Aslanian R, Madison VS (2008) Induced-fit docking of mometasone furoate and further evidence for glucocorticoid receptor 17α pocket flexibility. J Mol Graph Model 27:512–521

Yun CH, Boggon TJ, Li Y, Woo S, Greulich H, Meyerson M, Eck MJ (2007) Structures of lung cancer-derived EGFR mutants and inhibitor complexes: mechanism of activation and insights into differential inhibitor sensitivity. Cancer Cell 11:217

Zhan YH (1994) China Shennongjia resources of medicinal plants. Hubei Scientific and Technological Press, Wuhan

Zhong H, Tran LM, Stang JL (2009) Induced-fit docking studies of the active and inactive states of protein tyrosine kinases. J Mol Graph Model 28:336–346

Zou K, Wang JZ, Du M, Li Q, Tu GZ (2006) A pair of diastereoisomeric steroidal saponins from cytotoxic extracts of *Tupistra chinensis* Rhizomes. Chem Pharm Bull 54(10):1440–1442

Zou K, Wang JZ, Guo ZY, Du M, Wu J, Zhou Y (2009) Structural elucidation of four new furostanol saponins from *Tupistra chinensis* by 1D and 2D NMR spectroscopy. Magn Reson Chem 47:87–91